Co-published by
Institute of Fluid-Flow Machinery
Polish Academy of Sciences
Committee on Thermodynamics and Combustion
Polish Academy of Sciences

http://www.imp.gda.pl/archives-of-thermodynamics/

Parametric multi-response optimisation of various organic Rankine cycle configurations for geothermal heat source application using Taguchi – grey relational analysis

Dodeye Ina Igbong[a*], Mafel Obhuo[b], Oku Ekpenyong Nyong[a]

[a]University of Cross River State, Calabar, Cross River State, Nigeria
[b]Nigeria Maritime University, Okerenkoko, Delta State, Nigeria
*Corresponding author email: d.i.igbong@unicross.edu.ng

Received: 31.05.2023; revised: 6.12.2023; accepted: 19.04.2024

Abstract

In this study, statistical methods (Taguchi, analysis of variance (ANOVA), and grey relational analysis (GRA)) are used to evaluate the impact, contribution ratios, and order of importance of parameters on the energy and exergy efficiencies of the simple organic Rankine cycle (SORC) and dual pressure organic Rankine cycle (DORC). The parameters being investigated are the working fluid (A), pinch point temperature difference of the evaporator (B) and condenser (C), degree of superheating (D), evaporator temperature (E), condenser temperature (F), turbine isentropic efficiency (G), pump isentropic efficiency (H), and low-pressure evaporator temperature (J, for DPORC only). Whereas the Taguchi method determines the optimum parameter combination for maximum system performance, ANOVA weighs the influence of individual parameters on the performance of the target function, and GRA optimizes the multi-response characteristic function. The condenser and evaporator temperatures, pinch point temperature difference of the condenser and turbine isentropic efficiency are revealed as the major process parameters for multi-response performance characteristics of SORC, with an influence factor of 44.79%, 20.96%, 14.81% and 10.69%, respectively. While considering three different working fluids: HFE7000 (1), R245fa (2), and R141b (3), the combination $A_3B_2C_1D_1E_3F_1G_3H_3$ is determined as the optimum operating condition for multi-response performance characteristic of SORC with first- (energy) and second- (exergy) law efficiencies calculated as 18.64% and 51.69%, respectively. For DPORC, the turbine isentropic efficiency, condenser temperature, and pinch point temperature difference of the condenser and evaporator are the main process parameters for multi-response performance with 41.90%, 17.80%, 14.75%, and 10.47% impact factors, respectively. The best operating condition is obtained as $A_1B_1C_1D_3E_2F_1G_3H_3J_2$ with first- and second-law efficiencies computed as 13.17% and 57.33%, respectively.

Keywords: ANOVA; Dual pressure ORC; First- and second-law efficiencies; Grey relational analysis; Simple ORC; Taguchi.

Vol. 45(2024), No. 2, 231–246; doi: 10.24425/ather.2024.150868

Cite this manuscript as: Igbong, D.I., Obhuo, M., & Nyong, O.E. (2024). Parametric multi-response optimisation of various organic Rankine cycle configurations for geothermal heat source application using Taguchi-Grey Relational Analysis. *Archives of Thermodynamics*, 45(2), 231–246.

1. Introduction

The increased awareness of energy and environmental sustainability has spurred research interest in developing efficient and more environmentally friendly energy systems. Organic Rankine cycles (ORCs) are considered one of those technologies with promising potential for effective low-grade heat-to-electricity conversion, with wide application in exhaust waste heat

Nomenclature

$\dot{E}x$ – exergy, W
$\dot{E}x_D$ – exergy destruction, W
h – specific enthalpy, J/kg
h_0 – specific enthalpy at the reference state, J/kg
$\dot{m}$ – mass flow rate, kg/s
P – pressure, Pa
$\dot{Q}$ – heat rate, W
s – specific entropy, J/(kg K)
s_0 – specific entropy at a reference state, J/(kg K)
T – temperature, K, °C
w_A – actual enthalpy change in the turbine, J/kg
w_S – isentropic enthalpy change in the turbine, J/kg
$\dot{W}_{pump}$ – power to drive pump
$\dot{W}_{net,SORC}$ – net power of simple organic Rankine cycle, W
$\dot{W}_{net,DPORC}$ – net power of dual pressure organic Rankine cycle, W
$\dot{W}_{turb}$ – power produced from the turbine, W

Greek symbols

η – efficiency

Subscripts and Superscripts

ch – chemical
cond – condenser
cw – cooling water
ex – exergy
evap – evaporator
f – working fluid
heat – heat source
HP – high-pressure
in – inlet
IN – input
LP – low-pressure
out – outlet
pp – pinch point
PreH – preheater
Sat – saturation
SupH – superheater
sys – system
th – thermal
w – geothermal water

Abbreviations and Acronyms

ANOVA – analysis of variance
DOF – degree of freedom
DPORC – dual pressure organic Rankine cycle
GRA – grey relational analysis
GRG – grey relational grade
SORC – simple organic Rankine cycle

recovery, geothermal, solar, and biomass for electricity generation [1]. Instead of steam, it uses low-temperature organic working fluid, which makes it more flexible with good matching characteristics between a wide temperature range of heat sources and its working fluid, hence decreasing exergy losses in the evaporator and consequently improving the overall cycle exergy efficiency [2,3].

There are many studies in the literature that conduct analysis on the thermal and exergy efficiency performance of ORC. Some of them have focused on experimental and theoretical studies of ORC performance enhancement, while others have reported on the effect of different configurations on system performance.

In general, the ORC system has been widely utilised for electricity generation from low- and medium-temperature geothermal wells. Igbong et al. [1] performed an exergo-economic and optimization study of dual pressure ORC (DPORC) utilising geothermal sources. In that study, the system optimised for maximum efficiency obtained an exergy efficiency and a cost per unit exergy of 33% and 3.059 cent/kWh, respectively. Yamankaradeniz et al. [4] investigated the energy and exergy performance of ORC with an internal heat exchanger. The study assessed the effects of evaporator temperature and heat exchanger effectiveness on the operation of the ORC system and concluded that a maximum increase of 6.21% in exergy efficiency is achievable depending on the working conditions. Igbong et al. [5] carried out a comparative exergetic analysis of selecting working fluid for various operating conditions of simple and recuperative organic Rankine cycles. Sadeghi et al. [6] performed a comparative thermodynamic analysis of different ORC configurations (simple ORC (SORC), series two-stage ORC (STORC) and parallel two-stage ORC (PTORC)) using zeotropic mixtures and powered by a geothermal heat source of 100 C. The result revealed that STORC has better net power output when R407A refrigerant is used. Other interesting and useful pieces of literature on ORC systems utilising geothermal sources are those of Liu et al. [7], Mokhtari et al. [8], Sun et al. [9] and Zare [10].

The low- and medium-temperature waste heat from plants and industrial processes is being recovered and utilised by the ORC system to generate electricity [11–13]. Mansoury et al. [11] analyzed a two-stage ORC driven by waste heat recovered from the exhaust gas and cooling water from an engine operating under three modes. The authors carried out a parametric analysis to ascertain how parameters affect the energetic and exergetic performance of the system. Scardigno et al. [14] examined solar thermal ORC systems and optimised the design parameters to obtain maximum efficiencies (first and second law), and minimum cost of energy. The study revealed that the R32-based ORC system demonstrated higher performance over the R143a-based system for energy efficiency but lower for second-law efficiency. The performance and power produced by the ORC are directly affected by the system's operating condition. Moloney et al. [15] analyzed the effects of different turbine inlet temperatures and pressures on the performance of a supercritical ORC system. In that investigation, the system's first- and second-law performance was assessed using various refrigerants, and the system was optimised for maximum thermal and exergy efficiencies, including net output power. Many researchers have recently conducted parametric studies and optimization of ORC systems to improve their thermodynamic performance [16–18]. Wang et al. [18] investigated the effect of an increase in turbine inlet temperature on the ORC first- and second-law efficiencies,

net output power, and turbine sizing factor. A parametric study of the ORC was also performed using several hydrofluoroether refrigerants (HFE7500, HFE7100 and HFE7000) at the same operational conditions. Their results revealed that the HFE7000 showed better performance with regard to the first-law efficiency and net output power. Li [16] analyzed the performance of various ORC system configurations and computed the mass flow rate requirement for a 30kW turbine work ORC system using the energetic and exergetic approaches. The assessment suggested that the condenser temperature had a greater impact on the system's thermal efficiency than the evaporator temperature and the exergy destruction appeared to be in the region of low thermal efficiency.

The present study aims at utilising statistical methods for the optimisation of the first- and second-law efficiencies of different ORC system configurations. To effectively optimise the system's objective functions (performance or/and cost), the optimum parameter combination and impact of weight of an individual parameter must be established statistically. According to the literature, the Taguchi technique and the analysis of variance (ANOVA) method are widely used [19–21]. Bademlioglu et al. [19] utilised the Taguchi and ANOVA methods to investigate the optimum parameter combination and the impact of individual factors on the ORC thermal efficiency. In that study, the evaporator temperature, evaporator's pinch point temperature difference, superheating temperature, condenser's pinch point temperature difference, condenser temperature, turbine and pump isentropic efficiencies, and heat exchanger effectiveness were selected as the operating parameters and their weight on the cycle thermal efficiency were evaluated. The analysis concluded that three parameters (evaporator and condenser temperature, and turbine isentropic efficiency) account for 70% of the total impact ratio, and the best and worst operating conditions obtained produced a thermal efficiency of 18.1% and 9.6%, respectively. In another study, Kumar and Karimi [21] used the Taguchi and ANOVA techniques to obtain the optimum parameter combinations for optimising the energetic performance of the ORC, and the level of importance of individual parameters. Although these methods are well-established and widely used in other areas [22–25], only a few studies have been published on the application for ORC system performance improvement.

Whereas Taguchi and ANOVA techniques are deployed to obtain statistically optimum performance of a system, they are limited to linear objective functions and cannot determine the optimum parameter combinations for multi-response performance characteristics. Grey relational analysis (GRA) is another statistical method capable of evaluating multiple objective functions at the same time [20,27,28]. Bademlioglu et al. [20] performed a multi-objective parametric optimisation of ORC using the Taguchi-GRA method. In their study, the energetic and exergetic performance of the ORC were simultaneously optimised statistically. The multi-response performance characteristic of ORC was shown to be most influenced by the evaporator temperature, turbine efficiency, the effectiveness of the heat exchanger and condenser temperature, with an impact ratio of 31.37%, 19.53%, 16.64% and 16.61%, respectively. The best operating conditions for the multi-response performance of the ORC were calculated as 18.1% and 65.52% for the first and second-law efficiencies, respectively.

In the present study, parametric multi-response optimisation of various ORC configurations is evaluated and a comparative analysis is performed. The Taguchi-GRA statistical method is utilised to simultaneously optimise the first and second-law efficiencies, the contribution ratio of individual parameters, and the best parameter combination on the multi-response performance characteristics of different ORC configurations. The main contribution and benefit of this study can be summarized as follows:

- Perform multi-objective performance optimisation of different ORC configurations (SORC and DPORC) using statistical methods;
- Obtain the best parameter combination (operating conditions) for the multi-response performance characteristics and carry out a comparison of different ORC configurations;
- Investigate the impact of ORC configuration on the parameter contribution ratio to the multi-response performance characteristics of ORC.

2. Materials and methods

2.1. Description of system

Figures 1 and 2 show the schematic diagrams of the simple and dual pressure ORCs, respectively, for geothermal heat source utilization for electricity production. For the simple ORC (Fig. 1), the organic refrigerant fluid leaving the condenser (state 1) is compressed by the pump to the evaporator pressure (state 2). The fluid enthalpy is then increased in the preheater before entering the evaporator (state 3) as saturated liquid and exiting from it (state 4) as a saturated vapour. Geothermal heat is also used to superheat the saturated vapour in the superheater (state 5). The working fluid then undergoes expansion to condenser pressure in the turbine (state 6) and it is cooled in the condenser by the cooling water (state 7) into liquid (state 1).

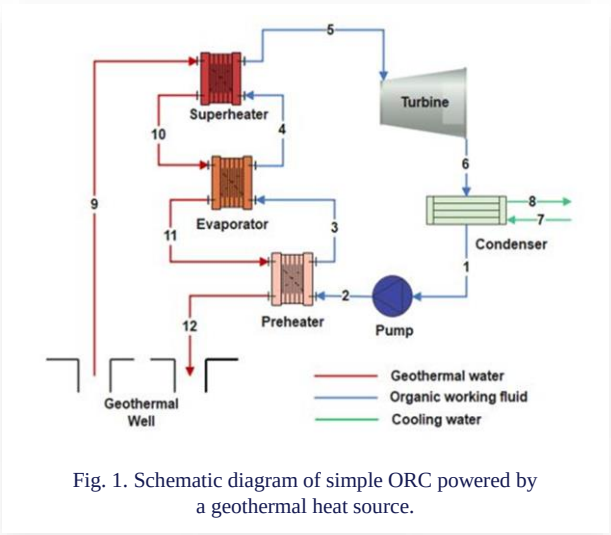

Fig. 1. Schematic diagram of simple ORC powered by a geothermal heat source.

In the dual pressure ORC (Fig. 2), after the refrigerant is pressurized in the low-pressure (LP) pump to LP evaporator pressure (P_{LP}) (state 2), the fluid flows through the preheater-1 where it is further heated and exits at P_{LP} saturated liquid temperature (state 3). The refrigerant flow is then divided into two parts. One part of the fluid is further compressed to high-pressure (HP) evaporator pressure in the (HP) pump (state 3b), while

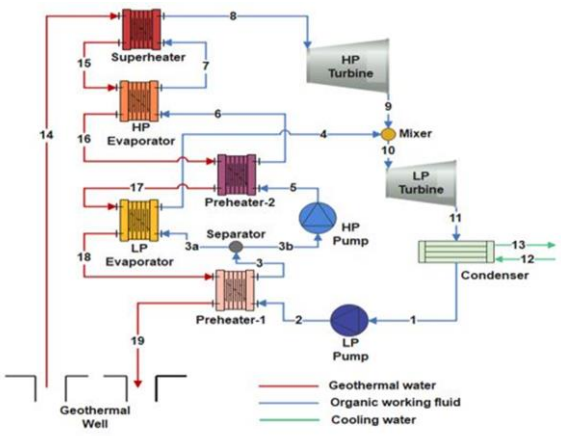

Fig. 2. Schematic diagram of dual pressure ORC powered by a geothermal heat source; LP – low pressure, HP – high pressure.

the other is transferred to the LP evaporator (state 3a). The high-pressure fluid exiting the HP pump (state 5) is channelled through preheater-2, where it absorbs heat before entering the HP evaporator (stage 6). Saturated liquid at P_{LP} temperature enters the HP evaporator and exits as saturated vapour (state 7). The fluid is further superheated before leaving the superheater (state 8) to be expanded in the HP turbine. The refrigerant exiting the HP turbine (state 9) mixes with the fluid from the LP evaporator (state 4) and then undergoes turbine expansion in the LP turbine (state 10). The working fluid vapour exiting the LP turbine (state 11) is condensed in the condenser by cooling water (state 12) into the liquid flow (state 1) exiting the condenser.

For the purpose of this study, to simplify the calculation, the following assumptions were adopted:

- The entire system undergoes steady-state flow conditions;
- Pressure drop and heat losses in the components are negligible;
- Changes in potential and kinetic energy are negligible;
- The range of values of parameters considered in the current study is based on an extensive literature survey by Bademlioglu et al. [20].

2.2. System modelling

Simple and dual-pressure ORC systems are modelled based on an energy and exergy balance at the system's component level. The performance calculation of the physical properties of the fluids utilised is achieved with the help of the Engineering Equation Solver (EES) [29].

2.2.1. Energy and exergy models

The mass and energy conservation relations, including the exergy balance equations for individual system components, are expressed as follows [30,31]:

$$\sum \dot{m}_{in} = \sum \dot{m}_{out}, \quad (1)$$

$$\sum \dot{m}_{in} h_{in} + \dot{Q}_{cv} - \sum \dot{m}_{out} h_{out} - \dot{W}_{cv} = 0, \quad (2)$$

$$\sum \dot{E}x_{in} - \sum \dot{E}x_{out} + \sum \dot{E}x_{heat} + \sum \dot{W}_J - \dot{E}x_{D,J} = 0, \quad (3)$$

where $\dot{m}$ represents mass flow rate, h is the specific enthalpy, $\dot{Q}_{cv}$ is the heat transferred and $\dot{W}_{cv}$ is the work rate. The quantities $\dot{E}x$ and $\dot{E}x_D$ stand for exergy and exergy destruction, respectively. Subscripts *in* and *out* refer to the inlet and outlet, respectively. Subscripts *heat* and *J* pertains to the heat source and *J*-th system component, respectively. The total exergy at each state point is the summation of the physical and chemical exergies when the potential and kinetic components are neglected. It can be expressed as [30]:

$$\dot{E}x = \dot{E}x_{ph} + \dot{E}x_{ch}. \quad (4)$$

The specific physical exergy is expressed as:

$$\dot{E}x_{ph} = \dot{m}[(h - h_0) - T_0(s - s_0)], \quad (5)$$

where s_0 and h_0 are the entropy and enthalpy at the reference state. The physical exergy determines the maximum useful work that can be done when the system state changes from the specific state *(T, P)* to the reference state *(T_0, P_0)*.

The net output power of the SORC and DPORC systems are defined as follows, respectively:

$$\dot{W}_{net,SORC} = \dot{W}_{turb} - \dot{W}_{pump}, \quad (6)$$

$$\dot{W}_{net,DPORC} = (\dot{W}_{HP_{turb}} + \dot{W}_{LP_{turb}}) - (\dot{W}_{HP_{pump}} + \dot{W}_{LP_{pump}}), \quad (7)$$

where $\dot{W}_{turb}$ is the power produced from the turbine and $\dot{W}_{pump}$ is the pump running power. Subscripts *HP* and *LP* refer to high pressure and low pressure, respectively.

The first-law (thermal) and second-law (exergy) efficiencies of the SORC system are defined as, respectively:

$$\eta_{th,SORC} = \frac{\dot{W}_{net,SORC}}{\dot{Q}_{IN}}, \quad (8)$$

$$\eta_{ex,SORC} = \frac{\dot{W}_{net,SORC}}{\dot{E}_{IN}}, \quad (9)$$

and for the DPORC system, they are expressed as:

$$\eta_{th,DPORC} = \frac{\dot{W}_{net,DPORC}}{\dot{Q}_{IN}}, \quad (10)$$

$$\eta_{ex,DPORC} = \frac{\dot{W}_{net,DPORC}}{\dot{E}_{IN}}, \quad (11)$$

where $\dot{Q}_{IN}$ and $\dot{E}_{IN}$ define the heat input and exergy input, respectively, for the SORC and DPORC systems from the geothermal heat source. The heat input $\dot{Q}_{IN}$ is equal to $\dot{Q}_9$ for SORC (Fig. 1) and $\dot{Q}_{14}$ for DPORC (Fig. 2).

The exergy input is defined as follows:

$$\dot{E}_{IN} = \dot{Q}_{IN}\left(1 - \frac{T_0}{T_{IN}}\right), \quad (12)$$

where T_{IN} represents the temperature of the stream at that state.

The energy and exergy equations for each component of the SORC and DPORC systems are shown in Table 1.

The thermodynamic models of SORC and DPORC systems used in this study were initially validated against literature data

[1,32–34]. The thermal efficiencies and evaporator and condenser temperatures of the systems are compared with those obtained from the literature and are presented in Table 2. Results reveal a good agreement between the present results obtained with those published in the literature.

Table 1. Energy and exergy destruction equations for individual components of the cycles.

Cycle	Component	Energy equations	Exergy destruction relations
SORC system	Superheater	$\dot{m}_{w,9}(h_9 - h_{10}) = \dot{m}_f(h_5 - h_4)$ $\dot{Q}_{SupH} = \dot{m}_{w,9}(h_9 - h_{10})$	$\dot{E}x_{D_{SupH}} = (\dot{E}x_9 + \dot{E}x_4) - (\dot{E}x_5 + \dot{E}x_{10})$
	Evaporator	$\dot{m}_{w,10}(h_{10} - h_{11}) = \dot{m}_f(h_4 - h_3)$ $\dot{Q}_{evap} = \dot{m}_{w,10}(h_{10} - h_{11})$	$\dot{E}x_{D_{evap}} = (\dot{E}x_{10} + \dot{E}x_3) - (\dot{E}x_4 + \dot{E}x_{11})$
	Turbine	$\eta_{turb} = \frac{w_A}{w_s} = \frac{h_5 - h_6}{h_5 - h_{6s}}$ $\dot{W}_{turb} = \dot{m}_f(h_5 - h_6)$	$\dot{E}x_{D_{turb}} = \dot{E}x_5 - (\dot{E}x_6 + \dot{W}_{turb})$
	Preheater	$\dot{m}_{w,11}(h_{11} - h_{12}) = \dot{m}_f(h_3 - h_2)$ $\dot{Q}_{PreH} = \dot{m}_{w,11}(h_{11} - h_{12})$	$\dot{E}x_{D_{PreH}} = (\dot{E}x_{11} + \dot{E}x_2) - (\dot{E}x_3 + \dot{E}x_{12})$
	Condenser	$\dot{m}_{w,8}(h_8 - h_7) = \dot{m}_f(h_6 - h_1)$ $\dot{Q}_{cond} = \dot{m}_f(h_6 - h_1)$	$\dot{E}x_{D_{cond}} = (\dot{E}x_6 + \dot{E}x_7) - (\dot{E}x_1 + \dot{E}x_8)$
	Pump	$\eta_{pump} = \frac{w_s}{w_A} = \frac{h_{2s} - h_1}{h_2 - h_1}$ $\dot{W}_{pump} = \dot{m}_f(h_2 - h_1)$	$\dot{E}x_{D_{pump}} = (\dot{E}x_1 + \dot{W}_{pump}) - \dot{E}x_2$
DPORC system	Superheater	$\dot{m}_{w,14}(h_{14} - h_{15}) = \dot{m}_f(h_8 - h_7)$ $\dot{Q}_{SupH} = \dot{m}_f(h_8 - h_7)$	$\dot{E}x_{D_{SupH}} = (\dot{E}x_7 + \dot{E}x_{14}) - (\dot{E}x_8 + \dot{E}x_{10})$
	HP Evaporator	$\dot{m}_{w,15}(h_{15} - h_{16}) = \dot{m}_f(h_7 - h_6)$ $\dot{Q}_{HP\_evap} = \dot{m}_f(h_7 - h_6)$	$\dot{E}x_{D_{HP\_evap}} = (\dot{E}x_{15} + \dot{E}x_6) - (\dot{E}x_{16} + \dot{E}x_7)$
	HP Turbine	$\eta_{turb} = \frac{w_A}{w_s} = \frac{h_8 - h_9}{h_8 - h_{9s}}$ $\dot{W}_{HP\_turb} = \dot{m}_f(h_8 - h_9)$	$\dot{E}x_{D_{HP\_turb}} = \dot{E}x_8 - (\dot{E}x_9 + \dot{W}_{HP\_turb})$
	Preheater 2	$\dot{m}_{w,16}(h_{16} - h_{17}) = \dot{m}_f(h_6 - h_5)$ $\dot{Q}_{PreH2} = \dot{m}_f(h_6 - h_5)$	$\dot{E}x_{D_{PreH2}} = (\dot{E}x_{16} + \dot{E}x_5) - (\dot{E}x_{17} + \dot{E}x_6)$
	HP Pump	$\eta_{HP\_pump} = \frac{w_s}{w_A} = \frac{h_{5s} - h_{3b}}{h_5 - h_{3b}}$ $\dot{W}_{HP\_pump} = \dot{m}_f(h_5 - h_{3b})$	$\dot{E}x_{D_{HP\_pump}} = (\dot{E}x_{3b} + \dot{W}_{HP\_pump}) - \dot{E}x_5$
	LP Evaporator	$\dot{m}_{w,17}(h_{17} - h_{18}) = \dot{m}_f(h_4 - h_{3a})$ $\dot{Q}_{LP\_evap} = \dot{m}_f(h_4 - h_{3a})$	$\dot{E}x_{D_{LP\_evap}} = (\dot{E}x_{17} + \dot{E}x_{3a}) - (\dot{E}x_4 + \dot{E}x_{18})$
	LP Turbine	$\eta_{turb} = \frac{w_A}{w_s} = \frac{h_{10} - h_{11}}{h_{10} - h_{11s}}$ $\dot{W}_{LP\_turb} = \dot{m}_f(h_{10} - h_{11})$	$\dot{E}x_{D_{LP\_turb}} = \dot{E}x_{10} - (\dot{E}x_{11} + \dot{W}_{LP\_turb})$
	Preheater 1	$\dot{m}_{w,18}(h_{18} - h_{19}) = \dot{m}_f(h_3 - h_2)$ $\dot{Q}_{PreH1} = \dot{m}_f(h_3 - h_2)$	$\dot{E}x_{D_{PreH1}} = (\dot{E}x_{18} + \dot{E}x_2) - (\dot{E}x_3 + \dot{E}x_{19})$
	LP Pump	$\eta_{pump} = \frac{w_s}{w_A} = \frac{h_{2s} - h_1}{h_2 - h_1}$ $\dot{W}_{LP\_pump} = \dot{m}_f(h_2 - h_1)$	$\dot{E}x_{D_{LP\_pump}} = (\dot{E}x_1 + \dot{W}_{LP\_pump}) - \dot{E}x_2$
	Condenser	$\dot{m}_{cw}(h_{13} - h_{12}) = \dot{m}_f(h_{11} - h_1)$ $\dot{Q}_{cond} = \dot{m}_f(h_{11} - h_1)$	$\dot{E}x_{D_{cond}} = (\dot{E}x_{12} + \dot{E}x_{11}) - (\dot{E}x_1 + \dot{E}x_{13})$

Table 2. Validation of parameters and cycle efficiencies.

Performance parameters for SORC/ DPORC	SORC						DPORC					
	Isobutane			R245fa			Isobutane			R245fa		
	Ref. [33]	Present study	Error %	Ref. [34]	Present study	Error %	Ref. [34]	Present study	Error %	Ref. [34]	Present study	Error %
T_{Sat_HP}	-	-	-	-	-	-	113.3	113.3	0.00	133.9	133.9	0.00
T_{Sat_LP}	96.53	96.53	0.00	112.9	112.9	0.00	76.60	76.60	0.00	86.80	86.8	0.00
P_{HP}	-	-	-	-	-	-	2530	2525	-0.197	2520	2516	-0.158
P_{LP}	1861.4	1859	-0.128	1670	1672	+0.119	1230	1251	+1.707	935	935	0.00
$\dot{m}_{HP}$	-	-	-	-	-	-	62.90	62.96	+0.095	141.7	142.4	+0.494
$\dot{m}_{LP}$	82.53	82.92	+0.472	181.8	182	+0.110	32.80	32.62	-0.548	62.20	62.10	-0.161
η_{th}	10.00	10.21	+2.10	12.17	12.31	+1.150	10.22	10.23	+0.097	12.51	12.25	-2.078
η_{sys}	5.97	6.052	+1.373	8.064	8.060	-0.049	7.066	7.032	-0.481	9.306	9.092	-2.299
$\dot{W}_{net}$	3269.9	3324	+1.654	5294	5301	+0.132	3871	3865	-0.154	6108	5984	-2.030

2.3. Methodology

2.3.1. Taguchi optimisation and analysis of S/N ratio

Taguchi optimisation is a design of experiment (DOE) technique that proposes an efficient approach to solving design problems and uses analysis of variance (ANOVA) to rank the order of importance of different factors for a given target function. In the present work, the Taguchi–Grey relational method is applied to simple ORC (SORC) and dual pressure ORC (DPORC) to optimise the parameter factors and levels and determine their order of importance for different ORC configurations.

Figure 3 shows a flow chart representing the application of Taguchi–Grey relational analysis for parametric optimisation of different ORC configurations. In this work, the performance characteristics for the first (N = 1) ORC configuration are initially calculated to obtain the cycle thermal and exergy efficiencies. Different control parameters, levels, and objective functions for the considered ORC configuration are identified. The orthogonal array table for the optimum trial runs is selected based on the number of parameters (factors), levels, and the total degree of freedom (DOF), which is the summation of each parameter's degree of freedom (DOF). For the SORC, Table 3 shows the number of factors and levels used for the analysis. Since there are eight factors with three levels, the total DOF is 25, which is the individual DOF number for each factor of each factor level minus one [20,35]. Therefore, the orthogonal array of L27 (3^8) is used for SORC analysis as shown in Tables 4 and 5. The results from each run, which are the first- and second-law efficiencies of the cycles, are transformed into the S/N ratios. The purpose of the S/N ratio calculation is to estimate the effect of the noise factors on the response and minimize that effect. There are three performance characteristics for calculating the S/N ratios; the lower is better, the nominal is best, and the higher is the better criteria [36]. Since the study seeks the maximization of both target functions (the first- and second-law efficiencies), the S/N ratio of higher is better (HB) is selected for this analysis:

$$\mathrm{S/N_{HB}} = -10\log\left(\frac{1}{n}\sum_{i=1}^{n} 1/y_i^2\right), \qquad (13)$$

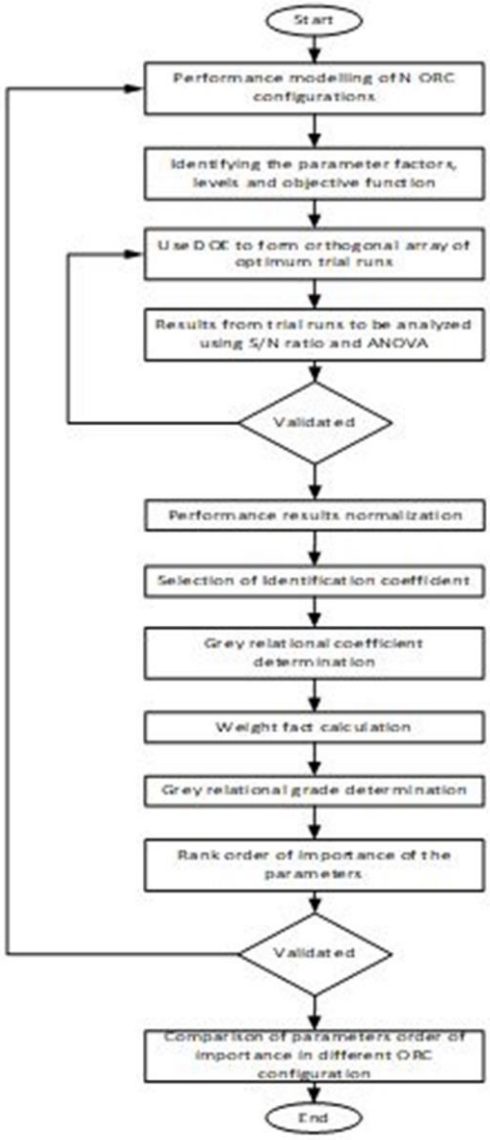

Fig. 3. Flow-chart for Taguchi – grey relational analysis.

Table 3. SORC and DPORC parameters and levels in the analysis.

SORC	DPORC	Parameters	Levels		
			1	2	3
A	A	Working fluid	HFE7000	R245fa	R141b
B	B	$\Delta T_{pp,evap}$	0	10	15
C	C	$\Delta T_{pp,cond}$	0	5	10
D	D	ΔT_{SH}	0	5	10
E	E	T_{evap}	110	130	150
F	F	T_{cond}	30	35	40
G	G	η_{turb}	0.75	0.8	0.85
H	H	η_{pump}	0.75	0.8	0.9
	J	$T_{LP,evap}$	75	80	85

where n refers to the number of cases, and y_i indicates the value of results for the i-th performance calculations.

The analysis of variance (ANOVA) is a good statistical tool for determining the contribution ratio to individual control parameters in the target functions. It is used alongside the Taguchi method to determine the contribution ratio and rank each parameter's significance.

2.3.2. Grey relational analysis

The Taguchi method is incapable of accurately determining the impact of parameters on multi-objective functions at the same time. Therefore, the grey relational analysis (GRA), which is more appropriate for achieving more than one target function simultaneously, is adopted in this study. There are six steps, as indicated in Fig. 3, and they enable the transformation of multi-response optimisation problems into single-response optimisation problems. The procedure begins with normalizing the analysis results of the target responses between the ranges of 0 and 1, also called grey relational generating.

The three common normalization procedures used are higher is better (HB), nominal is best (NB), and lower is better (LB) [26]. Since the aim of this study is the simultaneous maximization of the first- and second-law efficiencies, the HB criterion is selected as given:

$$y_i(k) = \frac{x_i^o(k) - \min x_i^o(k)}{\max x_i^o(k) - \min x_i^o(k)}, \tag{14}$$

where $y_i(k)$ refers to the normalised value of the response result, x^0 is the optimum value, and $\max x_i^o(k)$ and $\min x_i^o(k)$ represent the maximum and minimum values of $x_i^o(k)$, respectively.

After the identification coefficient ϕ has been selected, the grey relational coefficient (ξ_i) is then computed using equations:

$$\xi_i(k) = \frac{\Delta_{min} + \phi\Delta_{max}}{\Delta_{oi}(k) + \phi\Delta_{max}}, \tag{15}$$

$$\Delta_{oi}(k) = y_o(k) - y_i(k), \tag{16}$$

$$\Delta_{max} = \max_{\forall j \in i} \max_{\forall k} \left(y_o(k) - y_j(k) \right), \tag{17}$$

$$\Delta_{min} = \min_{\forall j \in i} \min_{\forall k} \left(y_o(k) - y_j(k) \right), \tag{18}$$

where $y_0(k)$ is the reference sequence, $y_i(k)$ is the comparative sequence, and Δ_{0i} is the difference between $y_0(k)$ and $y_i(k)$. Quantities Δ_{min} and Δ_{max} are the minimum and maximum values of Δ_{0i}, respectively. The value of the identification coefficient is in the range $0 < \phi < 1$ and is generally taken as 0.5. Grey relational coefficient (ξ_i) indicates the correlation between the target and actual normalized values [26].

Each factor/parameter of the objective function is weighted based on the degree of its influence on the first- and second-law efficiencies. For each response, the difference between the maximum and minimum values of each parameter's S/N ratio is known as *Delta* (see the fourth row in Table 5 and the fifth row in Table 7). The sum of the values of *Delta* for each parameter of each response is obtained (see the fifth row in Table 5 and the sixth row in Table 7). Then the weight factor is calculated as the ratio of the sum of the values of *Delta* from each parameter to the total value of *Delta* of the entire responses (see the seventh row in Tables 5 and 7) in accordance with the expression [37]:

$$w_i = \frac{\sum_{j=1}^{p} Delta_{ij}}{\sum_{i=1}^{m}\sum_{j=1}^{p} Delta_{ij}}, \tag{19}$$

where p is the number of parameters and m is the number of responses.

Finally, the grey relational grade (γ_i) for different weight factors, which indicates the degree of the relationship between the reference and comparative sequences is calculated. Since this study aims to maximize the first- and second-law efficiencies, the best result will correspond to the maximum grey relational grade.

The total grey relational grade for a given weight factor is expressed as follows:

$$\gamma_i = \frac{1}{2}\sum_{k=1}^{n} w_k \xi_i(k), \tag{20}$$

where n is the number of runs, w_k is the weight factor for k-th performance characteristics.

3. Results and discussion

As aforementioned, this work investigates the multi-parameter performance optimisation of SORC and DPORC, while simultaneously accounting for both the thermal and exergy efficiencies. The main aim of this work is to establish the order of importance and optimised parameter combination for both SORC and DPORC configurations and compare the results. The Taguchi method provides a quantitative impact of individual parameters on the cycle performance. The grey relational analysis (GRA) is then deployed for the optimisation of parameters affecting the cycles with multi-objective functions, such as thermal and exergy efficiencies. The parameters and levels of the SORC and DPORC are presented in Table 3. The L27 (3^8) and L27 (3^9) orthogonal arrays were designed for a standard three-level orthogonal array with 8 and 9 variables for SORC and DPORC, respectively. Tables 4 and 5 show 27 different cases with various combinations of factors in the orthogonal array. The analysis calculates the first- and second-law efficiencies for these cases, which are then transformed into S/N ratios, as shown in Tables 4 and 5.

Table 4. SORC L27 orthogonal array with their first and second-law efficiencies and S/N ratios.

	Parameters											
	A	B	C	D	E	F	G	H	Results		S/N Ratio	
Cases	Levels								η_{th}	η_{ex}	η_{th}	η_{ex}
1	1	1	1	1	1	1	1	1	11.53	62.11	-18.763	-4.137
2	1	1	1	1	2	2	2	2	12.99	59.82	-17.728	-4.463
3	1	1	1	1	3	3	3	3	14.20	58.45	-16.985	-4.664
4	1	2	2	2	1	1	1	2	10.84	60.63	-19.299	-4.346
5	1	2	2	2	2	2	2	3	12.37	58.52	-18.153	-4.654
6	1	2	2	2	3	3	3	1	13.35	57.03	-17.490	-4.878
7	1	3	3	3	1	1	1	3	10.16	59.23	-19.862	-4.549
8	1	3	3	3	2	2	2	1	11.56	57.14	-18.741	-4.861
9	1	3	3	3	3	3	3	2	12.74	55.80	-17.897	-5.067
10	2	1	2	3	1	2	3	1	12.40	53.60	-18.132	-5.417
11	2	1	2	3	2	3	1	2	11.82	50.83	-18.548	-5.878
12	2	1	2	3	3	1	2	3	15.33	51.02	-16.289	-5.845
13	2	2	3	1	1	2	3	2	11.63	57.31	-18.688	-4.835
14	2	2	3	1	2	3	1	3	11.17	54.70	-19.039	-5.240
15	2	2	3	1	3	1	2	1	14.07	55.14	-17.034	-5.171
16	2	3	1	2	1	2	3	3	13.26	55.11	-17.549	-5.175
17	2	3	1	2	2	3	1	1	12.36	52.04	-18.159	-5.673
18	2	3	1	2	3	1	2	2	15.76	52.35	-16.065	-5.622
19	3	1	3	2	1	3	2	1	10.85	49.55	-19.291	-6.099
20	3	1	3	2	2	1	3	2	15.47	50.55	-16.210	-5.926
21	3	1	3	2	3	2	1	3	14.49	47.90	-16.779	-6.393
22	3	2	1	3	1	3	2	2	12.49	48.88	-18.069	-6.217
23	3	2	1	3	2	1	3	3	17.12	50.33	-15.329	-5.963
24	3	2	1	3	3	2	1	1	15.72	47.31	-16.071	-6.501
25	3	3	2	1	1	3	2	3	11.70	50.86	-18.636	-5.872
26	3	3	2	1	2	1	3	1	16.18	51.67	-15.820	-5.735
27	3	3	2	1	3	2	1	2	15.01	48.75	-16.472	-6.241

Table 5. DPORC L27 orthogonal array with their first and second-law efficiencies and S/N ratios.

	Parameters												
	A	B	C	D	E	F	G	H	J	Results		S/N Ratio	
Case	Levels									η_{th}	η_{ex}	η_{th}	η_{ex}
1	1	1	1	1	1	1	1	1	1	11.14	58.10	-19.062	-4.716
2	1	1	1	1	2	2	2	2	2	11.99	58.46	-18.424	-4.662
3	1	1	1	1	3	3	3	3	3	11.94	59.77	-18.460	-4.470
4	1	2	2	2	1	1	1	2	2	10.30	57.62	-19.743	-4.788
5	1	2	2	2	2	2	2	3	3	10.91	58.57	-19.244	-4.646
6	1	2	2	2	3	3	3	1	1	8.382	62.34	-21.533	-4.104
7	1	3	3	3	1	1	1	3	3	9.627	57.09	-20.330	-4.868
8	1	3	3	3	2	2	2	1	1	8.938	59.67	-20.975	-4.484
9	1	3	3	3	3	3	3	2	2	7.179	63.83	-22.879	-3.899
10	2	1	2	3	1	2	3	1	2	11.76	50.83	-18.592	-5.877
11	2	1	2	3	2	3	1	2	3	10.63	49.97	-19.469	-6.025
12	2	1	2	3	3	1	2	3	1	11.98	50.76	-18.431	-5.889
13	2	2	3	1	1	2	3	2	3	11.01	53.18	-19.164	-5.485
14	2	2	3	1	2	3	1	3	1	9.009	52.35	-20.907	-5.621
15	2	2	3	1	3	1	2	1	2	10.40	52.57	-19.659	-5.585
16	2	3	1	2	1	2	3	3	1	12.11	51.62	-18.337	-5.743
17	2	3	1	2	2	3	1	1	2	10.16	50.54	-19.862	-5.927
18	2	3	1	2	3	1	2	2	3	11.23	51.05	-18.992	-5.840
19	3	1	3	2	1	3	2	1	3	10.09	46.24	-19.922	-6.699
20	3	1	3	2	2	1	3	2	1	12.38	47.43	-18.146	-6.478
21	3	1	3	2	3	2	1	3	2	9.545	45.54	-20.405	-6.832
22	3	2	1	3	1	3	2	2	1	11.02	45.80	-19.156	-6.782
23	3	2	1	3	2	1	3	3	2	13.95	47.70	-17.109	-6.429
24	3	2	1	3	3	2	1	1	3	10.54	45.48	-19.543	-6.843
25	3	3	2	1	1	3	2	3	2	10.40	46.64	-19.659	-6.624
26	3	3	2	1	2	1	3	1	3	13.21	48.02	-17.582	-6.371
27	3	3	2	1	3	2	1	2	1	7.719	44.56	-22.249	-7.021

To ensure the integrity of this study for both first and second-law analysis, the response table with average S/N ratios, the rank or order of importance of the parameters, and the graphs showing the parameter contribution ratios for SORC and DPORC are presented. Table 6 shows the average S/N ratios and parameter ranking (order of significance) on the SORC's first- and second-law efficiencies. The order of importance of parameters with regard to the first-law (thermal) efficiency is T_{evap} > working fluid > T_{cond} > η_{turb} > $\Delta T_{pp,\,cond}$ > η_{pump} > $\Delta T_{pp,evap}$ > ΔT_{SH}, and for the

Table 6. SORC average S/N ratios for the first and second-law efficiencies.

Parameters	First-law efficiency							
Levels	A	B	C	D	E	F	G	H
1	-18.32	-17.64	-17.19	-17.69	-18.70	-17.19	-18.11	-17.72
2	-17.72	-17.69	-17.65	-17.67	-17.53	-17.59	-17.78	-17.66
3	-16.96	-17.69	-18.17	-17.66	-16.79	-18.23	-17.12	-17.62
Delta (max-min)	1.36	0.05	0.98	0.03	1.91	1.05	0.99	0.10
Rank	2	7	5	8	1	3	4	6
$\sum Delta$	6.47							
Weight	68.66%							
	Second-law efficiency							
Levels	A	B	C	D	E	F	G	H
1	-4.624	-5.425	-5.380	-5.151	-5.183	-5.255	-5.440	-5.386
2	-5.428	-5.312	-5.430	-5.418	-5.377	-5.393	-5.423	-5.399
3	-6.105	-5.422	-5.349	-5.589	-5.598	-5.510	-5.296	-5.373
Delta (max-min)	1.481	0.113	0.080	0.438	0.415	0.255	0.144	0.026
Rank	1	6	7	2	3	4	5	8
$\sum Delta$	2.95							
Weight	31.33%							

Table 7. SORC ANOVA table for first- and second-law efficiency.

	Parameters	DOF	SS	MS	F	Contribution, %	DOF	SS	MS	F	Contribution, %
	First-law efficiency						Second-law efficiency				
A	Working fluid	2	8.3589	4.17944	474.60	21.34	2	9.8930	4.94649	8641.24	82.01
B	$\Delta T_{pp,evap}$	2	0.0160	0.00798	0.91	0.04	2	0.0745	0.03726	65.09	0.62
C	$\Delta T_{pp,cond}$	2	4.3294	2.16470	245.82	11.06	2	0.0297	0.01484	25.92	0.25
D	ΔT_{SH}	2	0.0031	0.00157	0.18	0.01	2	0.8767	0.43836	765.80	7.27
E	T_{evap}	2	16.7349	8.36746	950.18	42.73	2	0.7754	0.38768	677.25	6.43
F	T_{cond}	2	5.0378	2.51890	286.04	12.86	2	0.2935	0.14675	256.37	2.43
G	η_{turb}	2	4.5500	2.27499	258.34	11.62	2	0.1116	0.05578	97.45	0.92
H	η_{pump}	2	0.0437	0.02183	2.48	0.11	2	0.0031	0.00156	2.73	0.03
	Error	10	0.0881	0.00881		0.22	10	0.0057	0.00057		0.05
	Total	26	39.1618			100.00	26	12.0632			100.00

second-law (exergy) efficiency it is Working fluid > ΔT_{SH} > T_{evap} > T_{cond} > η_{turb} > $\Delta T_{pp,evap}$ > $\Delta T_{pp,cond}$ > η_{pump}, as shown in Table 6.

After the Taguchi analysis, analysis of variance (ANOVA) is performed to determine the contribution ratios of the parameters, and for the first-law efficiency, the parameters with the highest influence are found to be the evaporator temperature (E), working fluid (A), condenser temperature (F) and turbine efficiency (G), with contribution ratios of 42.73%, 21.34%, 12.73% and 11.62%, respectively, as presented in Table 7. The study concludes that the findings from the Taguchi and ANOVA methods are compatible with each other.

From Fig. 4, the optimum operating conditions are determined as working fluid = R141b (A_3), $\Delta T_{pp,evap}$ = 0°C (B_1), $\Delta T_{pp,\ cond}$ = 0°C (C_1), ΔT_{SH} = 10°C (D_3), T_{evap} = 150°C (E_3), T_{cond} = 30°C (F_1), η_{turb} = 85% (G_3) and η_{pump} = 90% (H_3), and under these conditions, the first-law efficiency of SORC is computed as 18.78%.

Similarly, the most effective parameters influencing the second-law efficiency of SORC are determined as working fluid, degree of superheating, evaporator temperature, and condenser temperature, with contribution ratios of 82.01%, 7.27%, 6.43% and 2.43%, respectively, as shown in Table 6. The optimum operating conditions for the second-law efficiency objective function of SORC are determined as working fluid = HFE7000 (A_1), $\Delta T_{pp,evap}$ = 5°C (B_2), $\Delta T_{pp,\ cond}$ = 10°C (C_3), ΔT_{SH} = 0°C (D_1), T_{evap} = 110°C (E_1), T_{cond} = 30°C (F_1), η_{turb} = 85% (G_3) and η_{pump} = 90% (H_3), as presented in Fig. 5. For these conditions (A_1 B_2 C_3 D_1 E_1 F_1 G_3 H_3), the second-law efficiency is calculated as 65.09%, which is clearly higher than the efficiencies of cases 1–27 (see Table 4). The contribution ratio or importance level of the different parameters on the target objective function, as determined by the ANOVA method, is presented in Table 6. It can be observed that the Taguchi and ANOVA methods are in complete agreement as regards the order of importance of the parameters. Indicating that the working fluid has the highest influence on the exergy efficiency with about 82.01%, ΔT_{SH}, T_{evap}, and T_{cond} have a total effect of 16.13%, and other parameters cumulatively account for 1.86% of the exergy efficiency.

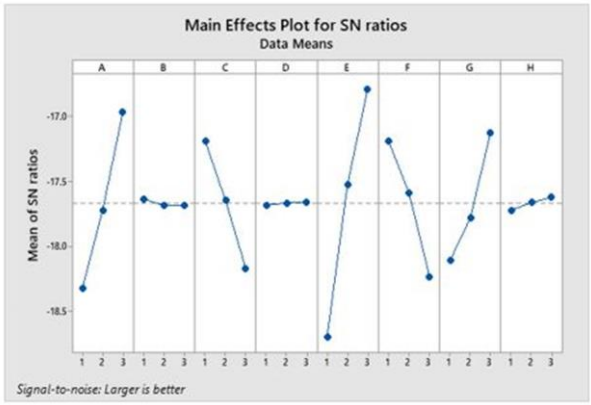

Fig. 4. Effect of each parameter on SORC first-law efficiency.

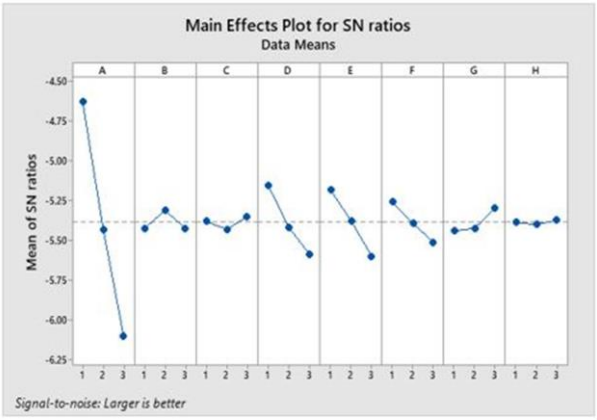

Fig. 5. Effect of each parameter on SORC second-law efficiency.

Table 8. DPORC average S/N ratios for the first- and second-law efficiencies.

Parameters	**First-law efficiency**								
Levels	A	B	C	D	E	F	G	H	J
1	-20.07	-18.99	-18.77	-19.46	-19.33	-18.78	-20.17	-19.64	-19.87
2	-19.27	-19.56	-19.61	-19.58	-19.08	-19.66	-19.38	-19.80	-19.59
3	-19.31	-20.10	-20.27	-19.61	-20.24	-20.21	-19.09	-19.21	-19.19
***Delta* (max-min)**	0.80	1.11	1.49	0.15	1.16	1.42	1.09	0.59	0.68
Rank	6	4	1	9	3	2	5	8	7
$\sum Delta$	8.49								
Weight	71.62%								
	Second-law efficiency								
Levels	A	B	C	D	E	F	G	H	J
1	-4.516	-5.739	-5.713	-5.618	-5.732	-5.663	-5.849	-5.623	-5.649
2	-5.777	-5.588	-5.706	-5.673	-5.628	-5.733	-5.691	-5.665	-5.625
3	-6.676	-5.642	-5.551	-5.678	-5.610	-5.573	-5.429	-5.681	-5.695
***Delta* (max-min)**	2.160	0.152	0.162	0.060	0.122	0.160	0.421	0.057	0.069
Rank	1	5	3	8	6	4	2	9	7
$\sum Delta$	3.363								
Weight	28.37%								

The Taguchi and ANOVA results of the DPORC system's parameters importance level are displayed in Tables 8 and 9, respectively. Result analysis indicates that the order of parameter influence on the DPORC first-law (thermal) efficiency is $\Delta T_{pp,cond} > T_{cond} > T_{evap} > \Delta T_{pp,evap} > \eta_{turb} >$ working fluid $> T_{LP,evap} > \eta_{pump} > \Delta T_{SH}$, and for the second-law (exergy) efficiency is working fluid $> \eta_{turb} > \Delta T_{pp,cond} > T_{cond} > \Delta T_{pp,evap} > T_{evap} > T_{LP,evap} > \Delta T_{SH} > \eta_{pump}$, as shown in Table 8.

As presented in Table 9, the parameters with the most significance on the first-law efficiency performance are $\Delta T_{pp,cond}$ (C), T_{cond} (F) and T_{evap} (E), with contribution ratios of 21.61%, 19.83% and 14.36%, respectively. For the second-law (exergy) efficiency, the parameters with significant influence are the working fluid (A) and turbine efficiency (G), with contribution ratios of 93.53% and 3.58%, respectively, and the other parameters cumulatively accounting for about 2.89%.

Table 9. DPORC ANOVA table for first- and second-law efficiency.

	Parameters	**DOF**	**SS**	**MS**	**F**	**Contribution, %**	**DOF**	**SS**	**MS**	**F**	**Contribution, %**
	First-law efficiency						Second-law efficiency				
A	Working fluid	2	3.696	1.8483	7.93	7.92	2	21.196	10.5981	585.55	93.53
B	$\Delta T_{pp,evap}$	2	5.508	2.7542	11.81	11.81	2	0.106	0.0531	2.94	0.47
C	$\Delta T_{pp,cond}$	2	10.088	5.0441	21.63	21.61	2	0.151	0.0756	4.18	0.67
D	ΔT_{SH}	2	0.106	0.0530	0.23	0.23	2	0.020	0.0102	0.56	0.09
E	T_{evap}	2	6.701	3.3503	14.37	14.36	2	0.078	0.0392	2.17	0.35
F	T_{cond}	2	9.254	4.6274	19.85	19.83	2	0.116	0.0580	3.20	0.51
G	η_{turb}	2	5.668	2.8442	12.15	12.15	2	0.811	0.4058	22.42	3.58
H	η_{pump}	2	1.688	0.8442	3.62	3.62	2	0.015	0.0079	0.44	0.07
J	$T_{LP,evap}$	2	2.084	1.0422	4.47	4.47	2	0.022	0.0111	0.62	0.10
	Error	8	1.865	0.2331		4.00	8	0.144	0.0181		0.64
	Total	26	46.661			100.00	26	22.662			100.00

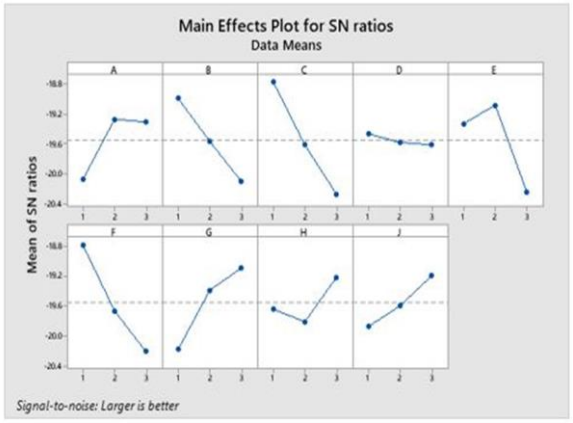

Fig. 6. Effect of each parameter on DPORC first-law efficiency.

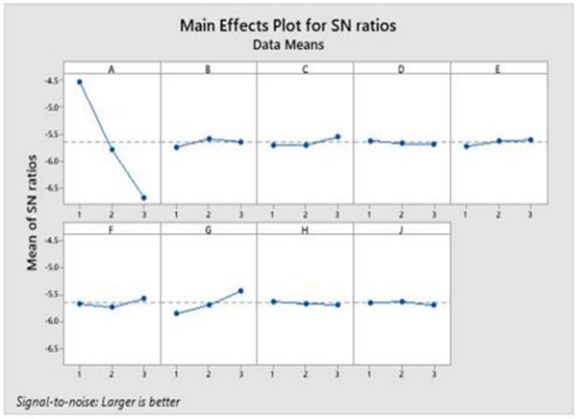

Fig. 7. Effect of each parameter on DPORC second-law efficiency.

The optimum operating condition of the DPORC system for maximum thermal and exergy efficiencies can be determined from Figs. 6 and 7, respectively. It is observed that the operating conditions of working fluid = R245fa (A_2), $\Delta T_{pp,evap}$ = 0°C (B_1), $\Delta T_{pp,cond}$ = 0°C (C_1), ΔT_{SH} = 0°C (D_1), T_{evap} = 130°C (E_2), T_{cond} = 30°C (F_1), η_{turb} = 85% (G_3) and η_{pump} = 90% (H_3), and $T_{LP,evap}$ = 85°C (J_3) produced the optimum first-law efficiency, and the operating conditions of working fluid = HFE7000 (A_1), $\Delta T_{pp,evap}$ = 10°C (B_2), $\Delta T_{pp,cond}$ = 10°C (C_3), ΔT_{SH} = 0°C (D_1), T_{evap} = 150°C (E_3), T_{cond} = 40°C (F_3), η_{turb} = 85% (G_3) and η_{pump} = 75% (H_1), and $T_{LP,evap}$ = 80°C (J_2) produced the optimum exergy efficiency of the DPORC system, as shown in Figs. 6 and 7, respectively. For the condition ($A_2B_1C_1D_1E_2F_1G_3H_3J_3$) the thermal efficiency is calculated as 14.64%, and for ($A_1B_2C_3D_1E_3F_3G_3H_1J_2$) the exergy efficiency is computed as 63.08%.

Up to this point in the analysis, the first- and second-law efficiencies have been optimised separately. However, to carry out the multi-response performance optimization, the grey relational

Table 10. Normalized results, grey relational coefficients, grey relational grade and order.

	SORC						DPORC					
Case	Normalized results		Grey relational coefficients		Grey relational grade	Order	Normalized results		Grey relational coefficients		Grey relational grade	Order
	η_{th}	η_{ex}	η_{th}	η_{ex}			η_{th}	η_{ex}	η_{th}	η_{ex}		
1	0.1968	1.0000	0.3837	1.0000	0.5767	8	0.5850	0.7026	0.5464	0.6270	0.5692	8
2	0.4066	0.8453	0.4573	0.7637	0.5532	9	0.7105	0.7213	0.6333	0.6421	0.6357	4
3	0.5733	0.7527	0.5395	0.6691	0.5800	6	0.7031	0.7893	0.6274	0.7035	0.6489	3
4	0.0977	0.9000	0.3566	0.8333	0.5059	13	0.4609	0.6777	0.4812	0.6081	0.5172	14
5	0.3132	0.7574	0.4213	0.6733	0.5002	14	0.5510	0.7270	0.5269	0.6468	0.5609	9
6	0.4583	0.6568	0.4800	0.5930	0.5154	12	0.1777	0.9227	0.3781	0.8661	0.5165	15
7	0.0000	0.8054	0.3333	0.7198	0.4544	19	0.3615	0.6502	0.4392	0.5884	0.4815	18
8	0.2011	0.6642	0.3849	0.5982	0.4517	20	0.2598	0.7841	0.4032	0.6984	0.4869	16
9	0.3707	0.5736	0.4428	0.5397	0.4731	17	0.0000	1.0000	0.3333	1.0000	0.5224	11
10	0.3218	0.4250	0.4244	0.4651	0.4371	21	0.6766	0.3254	0.6072	0.4257	0.5556	10
11	0.2385	0.2378	0.3964	0.3961	0.3963	25	0.5097	0.2807	0.5049	0.4101	0.4780	20
12	0.7428	0.2507	0.6603	0.4002	0.5787	7	0.7091	0.3217	0.6322	0.4243	0.5732	7
13	0.2112	0.6757	0.3880	0.6066	0.4564	18	0.5658	0.4473	0.5352	0.4750	0.5181	13
14	0.1451	0.4993	0.3690	0.4997	0.4099	23	0.2703	0.4043	0.4066	0.4563	0.4207	25
15	0.5618	0.5291	0.5329	0.5150	0.5272	11	0.4757	0.4157	0.4881	0.4611	0.4804	19
16	0.4454	0.5270	0.4741	0.5139	0.4865	16	0.7283	0.3664	06479	0.4411	0.5892	6
17	0.3161	0.3196	0.4223	0.4236	0.4227	22	0.4403	0.3103	0.4718	0.4203	0.4571	21
18	0.8003	0.3405	0.7146	0.4312	0.6257	3	0.5983	0.3368	0.5545	0.4298	0.5191	12
19	0.0991	0.1514	0.3569	0.3708	0.3612	27	0.4299	0.0872	0.4672	0.3539	0.4350	24
20	0.7629	0.2189	0.6783	0.3903	0.5880	5	0.7681	0.1489	0.6832	0.3701	0.5943	5
21	0.6221	0.0399	0.5695	0.3424	0.4983	15	0.3494	0.0509	0.4346	0.3450	0.4091	26
22	0.3348	0.1061	0.4291	0.3587	0.4070	24	0.5673	0.0644	0.5361	0.3483	0.4828	17
23	1.0000	0.2041	1.0000	0.3858	0.8075	1	1.0000	0.1629	1.0000	0.3739	0.8223	1
24	0.7989	0.0000	0.7132	0.3333	0.5941	4	0.4964	0.0477	0.4982	0.3443	0.4545	22
25	0.2213	0.2399	0.3910	0.3968	0.3928	26	0.4757	0.1079	0.4881	0.3592	0.4515	23
26	0.8649	0.2946	0.7873	0.4148	0.6705	2	0.8907	0.1796	0.8206	0.3787	0.6952	2
27	0.6968	0.0973	0.6225	0.3565	0.5391	10	0.0798	0.0000	0.3521	0.3333	0.3467	27

Table 11. SORC response table for grey relational grade.

Parameters								
Levels	A	B	C	D	E	F	G	H
1	-5.845	-6.016	-5.184	-5.748	-6.953	-4.653	-6.306	-6.057
2	-6.434	-5.778	-6.070	-6.112	-5.697	-6.029	-6.357	-6.030
3	-5.628	-6.113	-6.654	-6.047	-5.257	-7.225	-5.243	-5.820
Delta	0.806	0.336	1.470	0.365	1.696	2.572	1.114	0.237
Rank	5	7	3	6	2	1	4	8

Table 12. SORC ANOVA table for grey relational grade.

	Parameters	DOF	SS	MS	F	Contribution, %
A	Working fluid	2	3.1352	1.5676	13.43	4.71
B	$\Delta T_{pp,evap}$	2	0.5360	0.2680	2.28	0.81
C	$\Delta T_{pp,cond}$	2	9.8603	4.9301	41.96	14.81
D	ΔT_{SH}	2	0.6800	0.3400	2.89	1.02
E	T_{evap}	2	13.9512	6.9756	59.37	20.96
F	T_{cond}	2	29.8167	14.9084	126.88	44.79
G	η_{turb}	2	7.1188	3.5594	30.29	10.69
H	η_{pump}	2	0.3031	0.1515	1.29	0.46
	Error	10	1.1750	0.1175		1.76
	Total	26	66.5762			100.00

analysis (GRA) method is utilised to linearize the first and second-law efficiency target functions to a single multi-response performance function. As mentioned previously, the GRA method optimises the operating condition to obtain maximum first- and second-law efficiencies, simultaneously. The procedure for the GRA method is implemented as illustrated in the flowchart in Fig. 3, and the results, including order of importance, are shown in Table 10. The calculation of the weight factor of each target function (first- and second-law efficiency) has a strong effect in determining a realistic result of the multi-response performance and the grey relational grade (GRG). Based on Eq. (16), the weight factors of the first- and second-law efficiencies are 68.66% and 31.33% for SORC, and 71.62% and 28.37% for DPORC, respectively, as shown in Tables 6 and 8. Therefore, the equation of the grey relational grade (GRG) based on their weight factors for the SORC and DPORC systems can be expressed as, respectively:

$$\mathrm{GRG}_{SORC} = 0.6866\mathrm{GRC}_{\eta_{th,SORC}} + 0.3133\mathrm{GRC}_{\eta_{ex,SORC}}, \quad (21)$$

$$\mathrm{GRG}_{DPORC} = 0.7162\mathrm{GRC}_{\eta_{th,DPORC}} + 0.2837\mathrm{GRC}_{\eta_{ex,DPORC}} \quad (22)$$

where $\mathrm{GRC}_{\eta_{th,SORC}}$, $\mathrm{GRC}_{\eta_{ex,SORC}}$, $\mathrm{GRC}_{\eta_{th,DPORC}}$, $\mathrm{GRC}_{\eta_{ex,DPORC}}$ represent the first- and second-law efficiency's grey relational coefficients (GRCs) for SORC and DPORC systems, respectively.

The variation in grey relational grade (GRG) for the different multi-response performance cases (1 – 27) of the SORC and DPORC systems is illustrated in Table 10. It can be observed that case 23 ($A_3B_2C_1D_3E_2F_1G_3H_3$) and case 19 ($A_3B_1C_3D_2E_1F_3G_2H_1$) for the SORC system, and case 23 ($A_3B_2C_1D_3E_2F_1G_3H_3J_2$) and case 27 ($A_3B_3C_2\ D_1E_3F_2G_1H_2J_1$) for

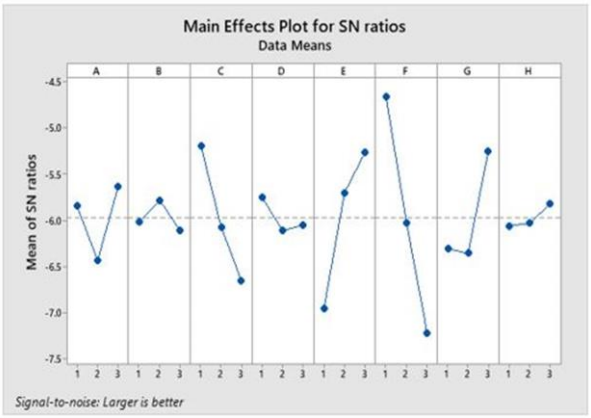

Fig. 8. Effect of each parameteron the multi-response characteristics for SORC system.

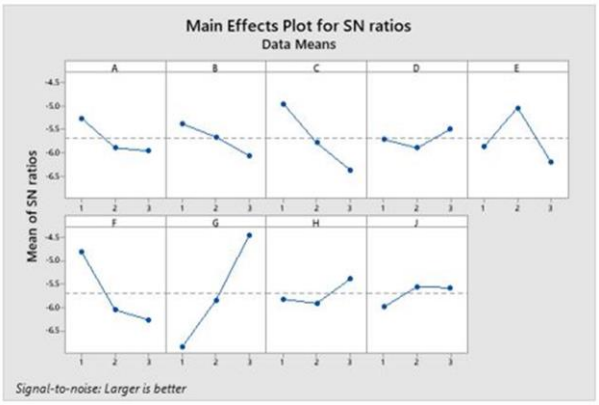

Fig. 9. Effect of each parameter on the multi-response characteristics for DPORC system.

the DPORC system, have the maximum and minimum values of GRG among cases 1 – 27, respectively.

From Figs. 8 and 9, the optimum parameter combinations for maximum first- and second-law efficiency (multi-response performance) for the SORC system are determined as working fluid = R141b (A_3), $\Delta T_{pp,evap}$ = 10°C (B_2), $\Delta T_{pp,cond}$ = 0°C (C_1), ΔT_{SH} = 0°C (D_1), T_{evap} = 150°C (E_3), T_{cond} = 30°C (F_1), η_{turb} = 85% (G_3) and η_{pump} = 90% (H_3), and for the DPORC system as working fluid = HFE7000 (A_1), $\Delta T_{pp,evap}$ = 0°C (B_1), $\Delta T_{pp,cond}$ = 0°C (C_1), ΔT_{SH} = 10°C (D_3), T_{evap} = 130°C (E_2), T_{cond} = 30°C (F_1), η_{turb} = 85% (G_3) and η_{pump} = 90% (H_3), and $T_{LP,evap}$ = 80°C (J_2). The first- and second-law efficiencies are calculated as 18.64% and 51.69% for SORC and 13.17% and 57.33% for DPORC, respectively, within these optimum conditions for the multi-response performance characteristics.

Furthermore, the response table for the grey relational grade (GRG) of SORC and DPORC systems is generated to determine the importance level of each parameter. For the SORC system, the order of importance of parameters is T_{cond} (44.79%) > T_{evap} (20.96%) > $\Delta T_{pp,cond}$ (14.81%) > η_{turb} (10.69%) > working fluid (4.71%) > ΔT_{SH} (1.02%) > $\Delta T_{pp,evap}$ (0.81%) > η_{pump} (0.46%), and the ANOVA results of the GRG of SORC are presented in Table 11 and 12. The order of importance of parameters for the multi-response performance characteristics of the DPORC system is η_{turb} > T_{cond} > $\Delta T_{pp,cond}$ > T_{evap} > working fluid > $\Delta T_{pp,evap}$ > η_{pump} > $T_{LP,evap}$ > ΔT_{SH}, as shown in Table 13, and with contribution ratios of 44.79%, 20.96%, 14.81%, 10.69%, 4.71%, 1.02%, 0.81% and 0.46%, respectively (Table 14**)**.

A comparison of parameter contribution ratios to the multi-performance characteristics for SORC and DPORC systems is shown in Figs. 10 and 11, respectively.

Table 13. DPORC response table for grey relational grade.

Parameters									
Levels	A	B	C	D	E	F	G	H	J
1	-5.257	-5.383	-4.950	-5.717	-5.871	-4.805	-6.835	-5.822	-5.987
2	-5.893	-5.662	-5.789	-5.899	-5.035	-6.048	-5.841	-5.907	-5.549
3	-5.961	-6.066	-6.373	-5.496	-6.205	-6.259	-4.436	-5.383	-5.576
Delta	0.704	0.683	1.423	0.403	1.170	1.454	2.399	0.524	0.437
Rank	5	6	3	9	4	2	1	7	8

Table 14. DPORC ANOVA table for grey relational grade.

	Parameters	DOF	SS	MS	F	Contribution, %
A	Working fluid	2	2.7170	1.3585	8.17	4.35
B	$\Delta T_{pp,evap}$	2	2.1208	1.0604	6.38	3.40
C	$\Delta T_{pp,cond}$	2	9.2062	4.6031	27.68	14.75
D	ΔT_{SH}	2	0.7335	0.3668	2.21	1.18
E	T_{evap}	2	6.5366	3.2683	19.66	10.47
F	T_{cond}	2	11.1119	5.5559	33.41	17.80
G	η_{turb}	2	26.1531	13.0766	78.64	41.90
H	η_{pump}	2	1.4245	0.7123	4.28	2.28
J	$T_{LP,evap}$	2	1.0819	0.5409	3.25	1.73
	Error	8	1.3302	0.1663		2.13
	Total	26	62.4158			100.00

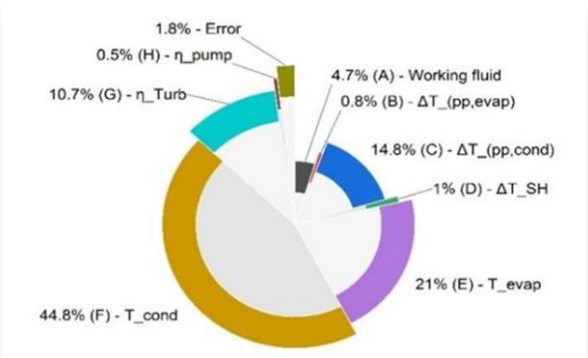

Fig. 10. Contribution ratio of each parameter to multi-response characteristics of SORC.

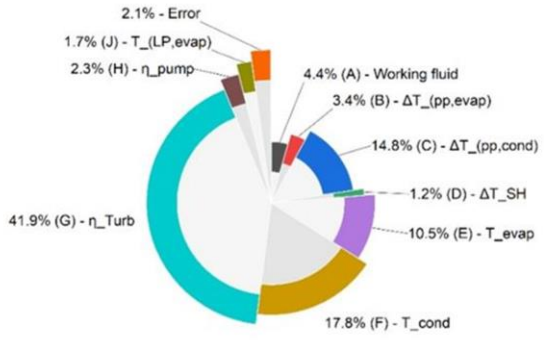

Fig. 11. Contribution ratio of each parameter to multi-response characteristics of DPORC.

4. Conclusions

This work uses the Taguchi–GRA method to optimise parameter combinations for maximum multi-response performance characteristics. The contribution ratios of parameters to the characteristics of SORC and DPORC systems are determined, and comparative analysis is performed. In this study, the fundamental parameters used for the analysis are working fluid, pinch

point temperature difference in the evaporator, pinch point temperature difference in the condenser, superheating temperature, evaporator temperature, condenser temperature, turbine and pump efficiencies for the SORC system. For the DPORC system, the LP turbine evaporation temperature is added to all parameters selected previously for SORC. The effects of these parameters on SORC and DPORC first and second law efficiencies are investigated. The grey relational analysis method is then deployed to linearize the first- and second-law efficiency functions to a single multi-response performance objective function, to determine the order of importance of these parameters and their contribution ratios to the multi-response performance process. It is worth noting, that the objective of this multi-response optimisation process is to optimise parameter combinations to simultaneously achieve an increase in the first and second-law efficiencies of SORC and DPORC systems.

Results obtained based on the methods discussed above are as follows:

- For the SORC system, the order of importance of the parameters on the first law (thermal) efficiency is T_{evap} > working fluid > T_{cond} > η_{turb} > $\Delta T_{pp,cond}$ > η_{pump} > $\Delta T_{pp,evap}$ > ΔT_{SH}, with the most significant parameters being found to be evaporator temperature (E), working fluid (A), condenser temperature (F) and turbine efficiency, with contribution ratios of 42.73%, 21.34%, 12.73% and 11.62%, respectively. The optimum operating condition determined is $A_3B_1C_1D_3E_3F_1G_3H_3$, which calculates the first-law (thermal) efficiency as 18.78%.
- The order of importance for the second law (exergy) efficiency is working fluid > ΔT_{SH} > T_{evap} > T_{cond} > η_{turb} > $\Delta T_{pp,evap}$ > $\Delta T_{pp,cond}$ > η_{pump}. The most effective parameters influencing the second-law efficiency of SORC are determined as working fluid, degree of superheating, evaporator temperature, and condenser temperature, with contribution ratios of 82.01%, 7.27%, 6.43% and 2.43%, respectively. The optimum operating conditions for the second-law efficiency objective function of SORC are determined as $A_1B_2C_3D_1E_1F_1G_3H_3$ with the second-law efficiency calculated as 65.09%.
- For the DPORC system, the parameters' level of importance on the thermal efficiency was determined as $\Delta T_{pp,cond}$ > T_{cond} > T_{evap} > $\Delta T_{pp,evap}$ > η_{turb} > working fluid > $T_{LP,evap}$ > η_{pump} > ΔT_{SH}, with the most influential parameters identified as $\Delta T_{pp,cond}$ (C), T_{cond} (F) and T_{evap} (E), with contribution ratios of 21.61%, 19.83% and 14.36%, respectively. The optimum condition observed was $A_2B_1C_1D_1E_2F_1G_3H_3J_3$ with an estimated cycle thermal efficiency of 14.64%.
- On the other hand, the order of importance of parameters for the second law (exergy) efficiency is working fluid > η_{turb} > $\Delta T_{pp,cond}$ > T_{cond} > $\Delta T_{pp,evap}$ > T_{evap} > $T_{LP,evap}$ > ΔT_{SH} > η_{pump}. The parameters with significant influence are the working fluid (A) and turbine efficiency (G), with contribution ratios of 93.53% and 3.58%, respectively, and other parameters cumulatively accounting for about 2.89%. An optimal exergy efficiency of 63.08% was obtained with the operating condition of $A_2B_2C_3D_1E_3F_3G_3H_1J_2$.
- The Grey relational analysis was implemented to simultaneously maximize both thermal and exergy efficiencies. For the SORC, the optimum operating condition for maximum first- and second-law efficiencies is $A_3B_2C_1D_1E_3F_1G_3H_3$, with 18.64% and 51.69% as the multi-response performance of the first- and second-law efficiency, respectively. For DPORC, 13.17% and 57.33% are the first- and second-law efficiency, respectively, obtained at the optimum operating condition of $A_1B_1C_1D_3E_2F_1G_3H_3J_2$.

Based on the analysis and thermodynamic comparison investigated in this study, SORC shows better thermal efficiency (+5.54%pt.) while DPORC represents a more advanced system in terms of exergy efficiency (+5.64%pt.). This could be attributed to the improved heat utilization due to the addition of LP turbine and heat exchangers (LP evaporator, Preheater 2, etc.). However, a more informed comparison will require the economic assessment of both systems, which is recommended for further research.

Acknowledgements

The authors appreciate the support of University of Cross River State under the 2023 Institution Based Research (IBR) project. This research project is funded by the Tertiary Education Trust Fund (TETFund) on the basis of the grant reference TETF/DR&D/CE/CRUTECH/IBR/2023/VOL.1.

References

[1] Igbong, D., Nyong, O., Enyia, J., Oluwadare, B., & Obhua, M. (2021). Exergoeconomic evaluation and optimization of Dual Pressure Organic Rankine Cycle (ORC) for geothermal heat source utilization. *Journal of Power and Energy Engineering*, 9(9), 19–40. doi: 10.4236/jpee.2021.99002

[2] Braimakis, K., & Karellas, S. (2018). Energetic optimization of regenerative Organic Rankine Cycle (ORC) configurations. *Energy Conversion and Management*, 159, 353–370. doi: 10.1016/j.enconman.2017.12.093

[3] Li, J., Ge, Z., Liu, Q., Duan, Y., & Yang, Z. (2018). Thermo-economic performance analyses and comparison of two turbine layouts for organic Rankine cycles with dual-pressure evaporation. *Energy Conversion and Management*, 164, 603–614. doi: 10.1016/j.enconman.2018.03.029

[4] Yamankaradeniz, N., Bademlioglu, A., & Kaynakli, O. (2018). Performance assessments of organic Rankine cycle with internal heat exchanger based on exergetic approach. *Journal of Energy Resources Technology*, 140, 102001–102008. doi: 10.1115/1.4040108

[5] Igbong, D., Nyong, O. E., Enyia, J., & Agba, A. (2021). Working fluid selection for simple and recuperative Organic Rankine Cycle operating under varying conditions : A comparative analysis. *Advances in Science and Technology Research Journal*, 15(4), 202–221. doi: 10.12913/22998624/142013

[6] Sadeghi, M., Nemati, A., & Yari, M. (2016). Thermodynamic analysis and multi-objective optimization of various ORC (organic Rankine cycle) configurations using zeotropic mixtures. *Energy*, 109, 791–802. doi: 10.1016/j.energy.2016.05.022

[7] Liu, Q., Chen, R., Yang, X., & Xiao, X. (2023). Thermodynamic analyses of sub- and supercritical ORCs using R1234yf, R236ea and their mixtures as working fluids for geothermal power generation. *Energies*, 16(15), 5676. doi: 10.3390/en16155676

[8] Mokhtari, H., Hadiannasab, H., Mostafavi, M., Ahmadibeni, A., & Shahriari, B. (2016). Determination of optimum geothermal Rankine cycle parameters utilizing coaxial heat exchanger. *Energy*, 102, 260–275. doi: 10.1016/j.energy.2016.02.067

[9] Sun, J., Liu, Q., & Duan, Y. (2018). Effects of evaporator pinch point temperature difference on thermo-economic performance of geothermal organic Rankine cycle systems. *Geothermics*, 75, 249–258. doi: 10.1016/j.geothermics.2018.06.001

[10] Zare, V. (2016). A comparative thermodynamic analysis of two tri-generation systems utilizing low-grade geothermal energy. *Energy Conversion and Management*, 118, 264–274. doi: 10.1016/j.enconman.2016.04.011

[11] Mansoury, M., Jafarmadar, S., & Khalilarya, S. (2018). Energetic and exergetic assessment of a two-stage organic Rankine cycle with reactivity controlled compression ignition engine as a low temperature heat source. *Energy Conversion and Management*, 166, 215–232. doi: 10.1016/j.enconman.2018.04.019

[12] Quoilin, S., Declaye, S., Tchanche, B. F., & Lemort, V. (2011). Thermo-economic optimization of waste heat recovery organic Rankine cycles. *Applied Thermal Engineering*, 31, 2885–2893. doi: 10.1016/j.applthermaleng.2011.05.014

[13] Roy, J. P., Mishra, M. K., & Misra, A. (2010). Parametric optimization and performance analysis of a waste heat recovery system using organic Rankine cycle. *Energy*, 35, 5049–5062. doi: 10.1016/j.energy.2010.08.013

[14] Scardigno, D., Fanelli, E., Viggiano, A., Bracco, G., & Magi, V. (2015). A genetic optimization of a hybrid organic Rankine plant for solar and low-grade energy sources. *Energy*, 91, 807–815. doi: 10.1016/j.energy.2015.08.066

[15] Moloney, F., Almatrafi, E., & Goswami, D. Y. (2017). Working fluid parametric analysis for regenerative supercritical organic Rankine cycles for medium geothermal reservoir temperatures. *Energy Procedia*, 129, 599–606. doi: 10.1016/j.egypro. 2017.09.216

[16] Li, G. (2016). Organic Rankine cycle performance evaluation and thermoeconomic assessment with various applications part I: Energy and exergy performance evaluation. *Renewable and Sustainable Energy Reviews*, 53, 477–499. doi: 10.1016/ j.rser. 2015.08.066

[17] Roy, J. P., & Misra, A. (2012). Parametric optimization and performance analysis of a regenerative Organic Rankine cycle using R123 for waste heat recovery. *Energy*, 39, 227–235. doi: 10.1016/j.energy.2012.01.026

[18] Wang, H., Li, H., Wang, L., & Bu, X. (2017). Thermodynamic analysis of organic Rankine cycle with hydrofluoroethers as working fluids. *Energy Procedia*, 105, 1889–1894. doi: 10.1016/j.egypro.2017.03.554

[19] Bademlioglu, A. H., Canbolat, A. S., Yamankaradeniz, N., & Kaynakli, O. (2018). Investigation of parameters affecting Organic Rankine Cycle efficiency by using Taguchi and ANOVA methods. *Applied Thermal Engineering*, 145, 221–228. doi: 10.1016/j.applthermaleng.2018.09.032

[20] Bademlioglu, A. H., Canbolat, A. S., & Kaynakli, O. (2020). Multi-objective optimization of parameters affecting Organic Rankine Cycle performance characteristics with Taguchi-Grey Relational Analysis. *Renewable and Sustainable Energy Reviews*, 117, 109483. doi: 10.1016/j.rser.2019.109483

[21] Kumar, U., & Karimi, M. N. (2014). Application of Taguchi's methods for optimizing organic Rankine cycle for recovering low grade industrial waste heat. *International Journal of Thermal & Environmental Engineering*, 8(2), 91–101. doi: 10.5383/ijtee. 08.02.005

[22] Kotcioglu, I., Cansiz, A., & Khalaji, M. (2013). Experimental investigation for optimization of design parameters in a rectangular duct with plate-fins heat exchanger by Taguchi method. *Applied Thermal Engineering*, 50, 604–613. doi: 10.1016/j.applthermaleng.2012.05.036

[23] Sahin, B. (2007). Taguchi approach for determination of optimum design parameters for a heat exchanger having circular-cross sectional pin fins. *Heat and Mass Transfer*, 45, 493–502. doi: 10.1007/s00231-006-0224-5

[24] Turgut, E., Cakmak, G., & Yildiz, C. (2012). Optimization of the concentric heat exchanger with injector turbulator by Taguchi method. *Energy Conversion and Management*, 53, 268–275. doi: 10.1016/j.enconman.2011.09.011

[25] Verma, V., & Murugesan, K. (2014). Optimization of solar assisted ground source heat pump system for space heating application by Taguchi method and utility concept. *Energy and Buildings*, 82, 296–309. doi: 10.1016/j.enbuild.2014.07.029

[26] Acir, A., Canli, M. E., Ata, I., & Cakiroglu, R. (2017). Parametric optimization of energy and exergy analyses of a novel solar air heater with grey relational analysis. *Applied Thermal Engineering*, 122, 330–338. doi: 10.1016/j.applthermaleng. 2017.05.018

[27] Chamoli, S., Yu, P., & Kumar, A. (2016). Multi-response optimization of geometric and flow parameters in a heat exchanger tube with perforated disk inserts by Taguchi grey relational analysis. *Applied Thermal Engineering*, 103, 1339–1350. doi: 10.1016/j.applthermaleng.2016.04.166

[28] Mia, M., Rifat, A., Tanvir, F., Gupta, M. K., Hossain, J., & Goswami, A. (2018). Multi-objective optimization of chip-tool interaction parameters using Grey-Taguchi method in MQL-assisted turning. *Measurement*, 129, 156–166. doi: 10.1016/ j.measurement.2018.07.014

[29] Klein, S. A. (2020). *Engineering Equation Solver* (V10.801-3D). F-Chart Software.

[30] Bejan, A., Tsatsaronis, G., & Moran, M. (1996). *Thermal Design & Optimization*. John Wiley & Sons Inc.

[31] Igbong, D. (2022). Energy and Exergy-based Performance Analysis of a Combined Recompression Supercritical Carbon Dioxide-Organic Rankine Cycle for Waste Heat Recovery. *Cleaner Energy Systems*, 100022. doi: 10.1016/j.cles. 2022.100022

[32] Delgado-Torres, A. M., & García-Rodríguez, L. (2010). Analysis and optimization of the low-temperature solar organic Rankine cycle (ORC). *Energy and Buildings*, 51, 2846–2856. doi: 10.1016/j.enconman.2010.06.022

[33] Yari, M. (2010). Exergetic analysis of various types of geothermal power plants. *Renewable Energy*, 35(1), 112–121. doi: 10.1016/j.renene.2009.07.023

[34] Wang, M., Chen, Y., Liu, Q., & Yuanyuan, Z. (2018). Thermodynamic and thermo-economic analysis of dual-pressure and single pressure evaporation organic Rankine cycles. *Energy Conversion and Management*, 177, 718–736. doi: 10.1016/ j.enconman.2018.10.017

[35] Tutar, M., Aydin, H., Yuce, G., Yavuz, N., & Bayram, A. (2014). The optimisation of process parameters for friction stir spot-welded AA3003-H12 aluminium alloy using a Taguchi orthogonal array. *Material Design*, 63, 789–797. doi: 10.1016/ j.matdes.2014.07.003

[36] Ross, P. J. (1996). *Taguchi techniques for quality engineering* (second). McGraw Hill.

[37] Yan, J., & Li, I. (2013). Multi-objective optimization of miling parameters - the trade-offs between energy, production rate and cutting quality. *Journal of Cleaner Production*, 52, 462–471. doi: 10.1016/j.jclepro.2013.02.030